

Proceeding Paper

Additive Manufacturing in Construction—Implementing Powder-Bed Fusion of Metals Using a Laser (PBF-LB/M) and Shape Optimization in the Construction Design Process [†]

Johannes Diller ^{*}, Christina Radlbeck, Dorina Siebert, Jakob Blankenhagen, Drilon Gubetini , Florian Oberhaidinger and Martin Mensinger

Chair of Metal Structures, School of Engineering and Design, Technical University of Munich, 80333 Munich, Germany; c.radlbeck@tum.de (C.R.); dorina.siebert@tum.de (D.S.); jakob.blankenhagen@tum.de (J.B.); d.gubetini@tum.de (D.G.); f.oberhaidinger@tum.de (F.O.); mensinger@tum.de (M.M.)

* Correspondence: johannes.diller@tum.de

[†] Presented at the 15th International Aluminium Conference, Québec, QC, Canada, 11–13 October 2023.

Abstract: In this study, the implementation of the PBF-LB/M process into the construction design and building process was investigated. To this purpose, a tensegrity-tower was designed, planned, and built. The nodes between the compression rods and the tension cables were manufactured by PBF-LB/M/AlSi10Mg. Four different nodes were designed and shape-optimized by vertex-morphing. In order to qualify the tensegrity nodes according to the German regulations, mechanical as well as microstructural evaluations were conducted. Tensile tests of a manufactured tensegrity node in a fully hinged setup were carried out. Additionally, fatigue testing was conducted. The tensegrity nodes were heat-treated (T6) and subsequently vibratory ground to reduce the surface roughness. The results indicate that it is feasible to integrate the PBF-LB/M process into the design and construction process. The tower is now a permanent and tangible exhibit in the Deutsches Museum in Munich.

Keywords: powder bed fusion of metals using a laser; additive manufacturing; tensegrity tower; additive manufacturing in construction; AlSi10Mg; tensile testing; fatigue



Citation: Diller, J.; Radlbeck, C.; Siebert, D.; Blankenhagen, J.; Gubetini, D.; Oberhaidinger, F.; Mensinger, M. Additive Manufacturing in Construction—Implementing Powder-Bed Fusion of Metals Using a Laser (PBF-LB/M) and Shape Optimization in the Construction Design Process. *Eng. Proc.* **2023**, *43*, 10. <https://doi.org/10.3390/engproc2023043010>

Academic Editor: Houshang Alamdari

Published: 12 September 2023



Copyright: © 2023 by the authors. Licensee MDPI, Basel, Switzerland. This article is an open access article distributed under the terms and conditions of the Creative Commons Attribution (CC BY) license (<https://creativecommons.org/licenses/by/4.0/>).

1. Introduction

The powder bed fusion of metals using a laser (PBF-LB/M/AlSi10Mg) allows for the creation of complex geometries and intricate designs that would be difficult or impossible to achieve using traditional manufacturing methods. It is already widely used in the aerospace, automotive, and medical sectors. The application of the PBF-LB/M process in the construction sector, however, is a relatively new field. Yet, it has the potential to revolutionize the construction sector with its ability to create complex structures with implemented features like lightweight design by shape optimization. Now, the issue arises regarding the specific applications that require complex but easily adjustable structures. For instance, the roof of the exhibition halls in Milan exemplifies a remarkably intricate structure comprising 16,500 nodes. It is important to note that these nodes do not possess identical geometries, as illustrated in Figure 1. Similar instances can be observed in architectural masterpieces such as the roof of the Jewel Changi airport in Singapore or Waterloo Station in London just to name a few.

Typically, the design engineer is expected to exert significant effort in order to minimize the utilization of diverse node geometries. The capability of the PBF-LB/M process to facilitate the seamless production of complex structures grants designers the freedom to utilize node geometries as needed. This reduces the work of the design. Nonetheless, the PBF-LB/M process remains significantly time-consuming and incurs substantial costs in

comparison to conventional manufacturing methods. Consequently, it is imperative for the application of this manufacturing technique to be economically feasible.



Figure 1. Example of possible application for additive manufacturing [1].

The potential of additive manufacturing compared to conventional processes is based on two fundamental principles, which are depicted in Figure 2. The first principle is the design freedom offered by additive manufacturing. Unlike conventional methods, PBF-LB/M provides a greater opportunity to manufacture complex components without incurring additional costs. The second principle is the quantity dependency. Conventional processes often require a high number of components to generate low component costs. However, additive manufacturing processes such as PBF-LB/M exhibit only a small-scale effect. Since the pre-process is performed only once, a slight decrease in price can be observed even with a high number of components (refer to Figure 2). Therefore, it is possible to achieve low component costs even with a small number of components [2]. It must be mentioned that this graph does not include the cost of redesign. This would result in no decrease in cost per part vs. number of parts in Figure 2.

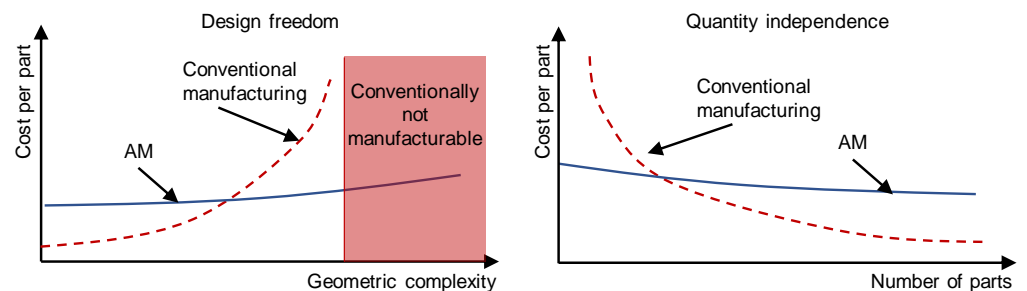


Figure 2. Potential of additive manufacturing (AM) vs. conventional manufacturing methods (e.g., CNC-machining, casting) in accordance to [2].

This is due to a significant dependency on fixed costs in conventional processes. Fixed costs primarily arise from the production of component-specific tooling (e.g., molds for casting). To make conventional manufacturing economically viable, the manufacturer must produce a large number of components to cover these fixed costs. In the case of a smaller quantity of components, additive manufacturing is usually more advantageous since it can be carried out without the need for tooling.

In this work, the implementation of the PBF-LB/M process, including the incorporation of shape optimization into the construction design, is investigated and evaluated. A tensegrity tower with a height of 5 m, consisting of 9 compression rods and 18 connecting nodes with four different initial geometries, was built, which can be seen in Figure 3. First, the global design of the tensegrity tower was carried out, followed by the local design of the connecting nodes between the cables and the compression rods. The four different initial geometries of the connection nodes were developed and shape-optimized using the

vertex-morphing technique [3]. The connecting nodes were subsequently manufactured by the PBF-LB/M process. After manufacturing, post-processing methods like T6-heat treatment, as well as vibratory grinding and polishing, were conducted. These methods will be further explained in the following chapter.

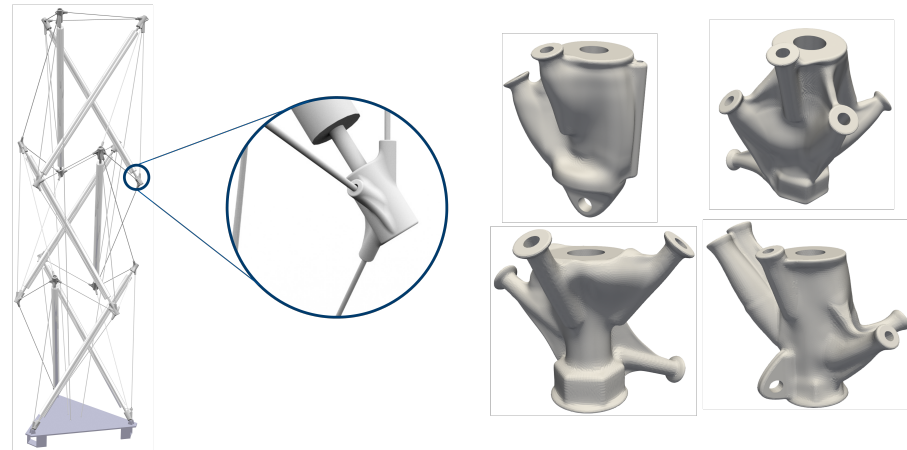


Figure 3. (Left): 3D-model of the tensegrity tower with close up of a connecting node (initial design); (Right): shape-optimized designs of the four different connecting nodes.

2. Materials and Methods

2.1. Design

Figure 4 provides an overview of the general methodology employed to integrate the PBF-LB/M process and its subsequent integration into the construction design.

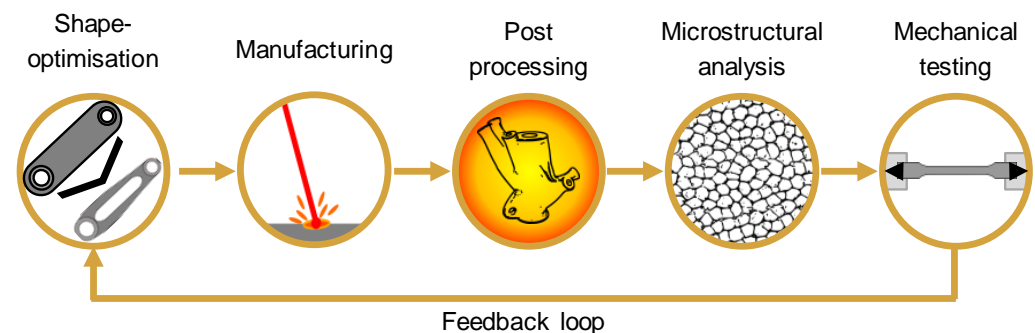


Figure 4. Workflow for the implementation of the PBF-LB/M process into the construction sector.

The overall design of the tensegrity tower was determined through the utilization of form finding techniques. Form finding in engineering is the process of determining the optimal shape and configuration of structural systems. It involves achieving equilibrium between internal forces and external loads while considering factors such as aesthetics, material properties, and construction feasibility. Methods include physical modeling, computational simulations, and optimization techniques. Form finding enables the creation of efficient and visually appealing structures that meet design criteria [4]. The software Rhinoceros 3D (Robert McNeel & Associates, Barcelona, Spain) with the Grasshopper plugin was employed for this purpose. The comprehensive structural analysis was performed utilizing the finite-element software SOFiSTiK (SOFiSTiK AG, Nuernberg, Germany). Subsequently, the obtained loads and loading directions of the cables at each connection node of the global structure were taken out and used for the local design process of the respective connection nodes, see Figure 3. The initial designs of each four nodes can be observed in Figure 3. The compression rods were connected to the nodes by using threaded rods. The attachment of the cables to the nodes was achieved using internal threads within the connection node. These internal threads were machined post-manufacturing, as the

likelihood of higher porosity in threads manufactured through PBF-LB/M is significant. Porosity can give rise to cracks under cyclic loading conditions [5].

Following the initial design, the connection nodes were shape optimized utilizing the vertex-morphing technique. For a comprehensive understanding of the vertex-morphing technique, refer to [6,7].

2.2. Manufacturing and Post-Processing

The applied material for the connection nodes was AlSi10Mg by TLS-Technik GmbH & Co. KG (Hartenstein, Germany). The chemical composition is presented in Table 1. A particle size of 20–63 μm was used. For the manufacturing process, a Realizer SLM 250 machine, outfitted with a 400 W pulsed laser, was used. The laser parameters employed during the manufacturing process of the connection nodes can be found in Table 2. The build platform temperature was set to 165 °C.

Table 1. Chemical composition of AlSi10Mg according to the manufacturer.

Element	Al	Si	Mg	Fe	Ti	Zn	Mn	Cu	Cr
wt.-%	Bal.	9–11	0.20–0.45	≤ 0.55	≤ 0.15	≤ 0.10	≤ 0.45	≤ 0.05	≤ 0.05

Table 2. Applied laser parameters for the manufacturing of the connection nodes.

Laser Parameter	Energy Density	Laser Power	Laser Speed	Hatch Distance	Layer Thickness
Value	80 J/mm ³	400 W	1000 mm/s	0.1 mm	0.05 mm

To investigate the mechanical properties, two additional build jobs were carried out. In each build job, five tensile specimens were manufactured for each building direction (0°, 45°, 90°). Additionally, three cubic specimens measuring 10 mm \times 10 mm \times 10 mm were produced for microstructural analysis. One of the build jobs was T6 heat-treated T6 as described below, while the other one remained in the as-built state.

After manufacturing, the connection nodes were heat-treated. A T6-heat treatment was applied using the parameters of [8]. The heating rate was set to 10 °C/min. Afterwards, a solution heat treatment was performed at 525 °C for a duration of 6 h. Following the solution heat treatment, the material was quenched. Finally, precipitation hardening was carried out at 165 °C for a period of 7 h. This not only supposedly improves the ductility, it also reduces the possible occurring residual stresses of the PBF-LB/M-manufactured parts [9].

After the completion of the heat treatment process, the nodes were cut from the build plate with a band saw, and the support structure was manually removed. To mitigate surface roughness, a three-step approach of vibratory grinding was employed. Initially, a coarse ceramic grinding material was employed for a duration of 24 h, succeeded by a finer ceramic grinding material for 4 h. The final step encompassed the utilization of fine polishing material for a period of two hours.

2.3. Mechanical Testing and Microstructural Investigation

To investigate the mechanical properties such as yield strength, ultimate tensile strength, and elongation at fracture, uniaxial tensile testing was carried out before and after the T6 heat treatment. Tensile testing was conducted using a Zwick and Roell Z100 tensile testing machine with a 100 kN load cell. To investigate the porosity and the microstructure, the aforementioned cubical specimens with a dimension of 10 mm \times 10 mm \times 10 mm were hot-embedded in epoxy resin, ground, and polished using a Struers CitoPress and a Struers LaboPol. The grinding parameters are shown in Table 3. The specimens were etched using hydrochloric acid (HCl) and nitric acid (HNO₃), known as aqua regia. The porosity was measured using a grey-scale comparison of the binarized and polished cubicals.

Table 3. Grinding parameters for surface treatment of the connection nodes.

Step	1	2	3	4
Grinding disk	MD Molto 220	MD Largo	MD Dac	MD Nap
Duration	4 min	4 min	4 min	3 min
Rev./min	150	150	150	150
Pressure	30 N	30 N	30 N	30 N
Lubricant	Water	6 μm	3 μm	1 μm

As the tensegrity tower is intended to serve as a permanent and tangible exhibit at the Deutsches Museum in Munich, the connection nodes are subjected to both static and cyclic loading. Thus, comprehensive static and cyclic tests were performed to evaluate the structural performance. The internal thread within the connection nodes emerged as the most critical region in terms of fatigue. Therefore, the threaded regions were cut from the tensegrity nodes so that a uni-axial fatigue test of the internal thread was able to be carried out. Two M12 threaded rods were connected to the specimen. The rods were subsequently clamped in the fatigue testing machine. The high cycle fatigue testing was conducted under ultimate limit state (ULS) loading conditions to assess its durability. The region of the internal threads was cut from the node and mounted into a uniaxial fatigue testing machine. An Instron 8032 fatigue testing machine with an Instron 8800 controller was used. The fatigue load was applied in a sinusoidal manner. The fatigue test was stopped at 1×10^7 cycles. The static testing of one complete node with real loading conditions is explained and assessed in [6].

3. Results

3.1. Static Mechanical Properties

Figure 5 displays the results of tensile tests conducted on specimens with various building directions (0° , 45° , and 90°) in both the as-built (AB) and T6 heat-treated states.

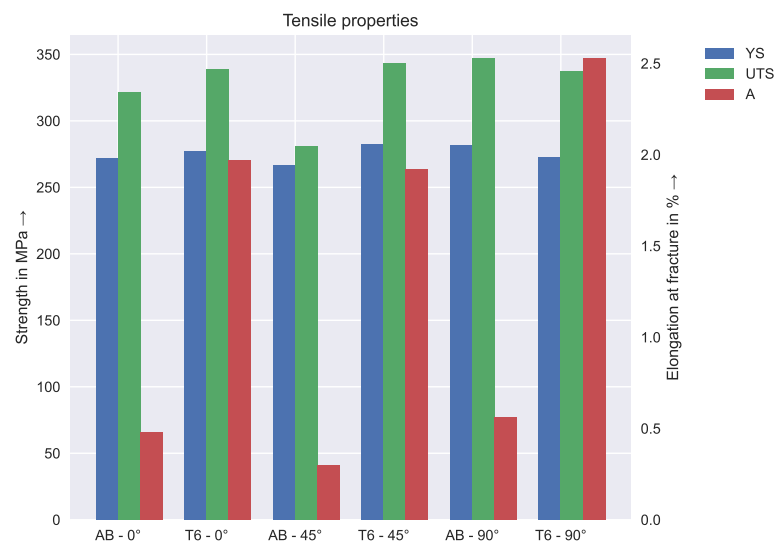


Figure 5. Results of tensile test in the as-built (AB) configuration and after T6 heat treatment (T6), with orientations of 0° , 45° , and 90° . YS: yield strength; UTS: ultimate tensile strength; and A: elongation at fracture.

Applying T6 heat treatment results in an observable increase in the elongation at fracture, whereas the yield strength and ultimate tensile strength show only marginal improvements. For safety considerations, the shape optimization and design of the connection nodes were based on the lowest recorded values of the T6 heat-treated specimens with

regard to the yield strength, the ultimate tensile strength, and the elongation at fracture. Here, the T6-0° condition was used.

3.2. Microstructure

Figure 6 shows the microstructure before and after the T6 heat treatment, with different magnifications.

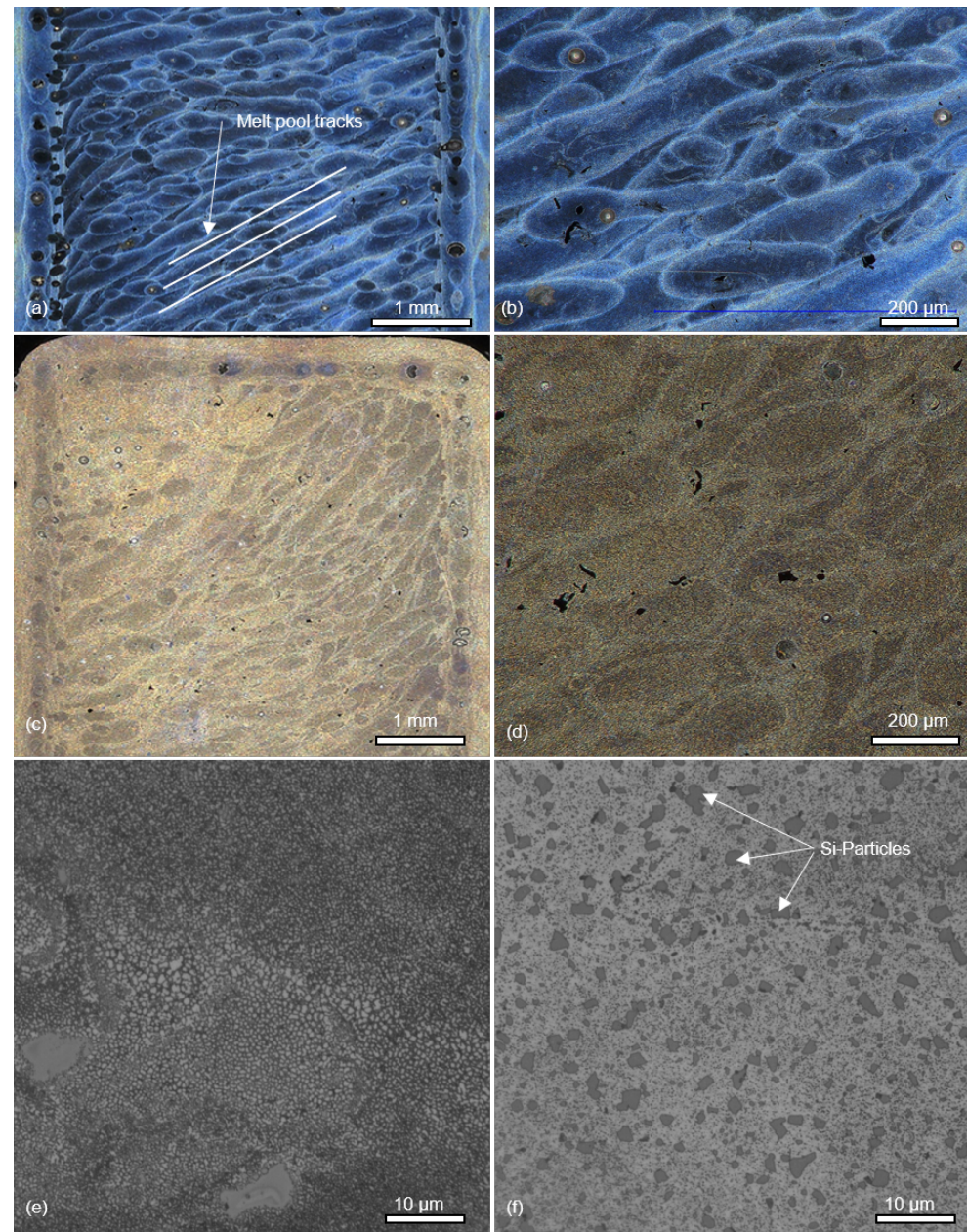


Figure 6. Microstructure of PBF-LB/M/AlSi10Mg before and after T6 heat treatment; (a,b) as-built microstructure, cross-sectional polish; (c,d) T6 heat-treated microstructure, cross-sectional polish; (e) as-built microstructure cross-sectional polish; and (f) T6 heat-treated microstructure showing Si-particles.

During T6 heat treatment of the AlSi10Mg alloy, Ostwald ripening occurs as smaller precipitates dissolve and redeposit onto larger ones, resulting in an increase in their size and a shift in the size distribution. This phenomenon enhances the strength and mechanical properties of the material by creating larger precipitates that act as barriers to dislocation movement. Moreover, the high-temperature aging process promotes the coalescence of Si

particulates in the alloy, facilitated by Ostwald ripening, where smaller Si particles dissolve and merge with larger ones, leading to the formation of larger Si agglomerates with improved mechanical properties [10]. The formation of the Si-particles can be seen in Figure 6, and the respective mechanical properties can be seen in Figure 5. The PBF-LB/M-manufactured parts exhibited a density of 99.94 %. This density is within the upper range of multiple other investigations [11–13].

3.3. Fatigue

The results of the fatigue testing with various loading scenarios are presented in Table 4. The presented data display the loads rather than the stresses; this is attributed to the heterogeneous cross-sectional profiles of the cut off specimens containing internal threads. It is evident that all the applied fatigue loads resulted in run-outs, meaning that no fractures occurred.

Table 4. Results of fatigue tests on four different specimens subjected to ultimate limit state (ULS) loads.

Specimen	ΔF (kN)	Min. F (kN)	Max. F (kN)	Stress Ratio	No. of Cycles
1	1.5	6	7.5	0.8	1×10^7
2	1.5	15	16.5	0.9	1×10^7
3	3.0	15	18	0.83	1×10^7
4	3.0	15	18	0.83	1×10^7

4. Discussion

The tensegrity tower was erected in the Deutsches Museum in Munich in June 2022. Since then, the tower has been a successful, educational exhibit. In summary, while the implementation of the PBF-LB/M process in construction design and assembly proves to be feasible (as can be seen in Figure 7), it requires careful attention to laser parameters, post-processing techniques, quality assurance, and addressing fatigue concerns, particularly in high porosity materials like AlSi10Mg. In addition to the previously stated considerations, the unique nature of each stage of PBF-LB/M manufacturing poses economic challenges when it comes to assessing and certifying each geometry. Conducting individual assessments for each unique part would be economically unfeasible. Porosity remains a significant issue, particularly in relation to fatigue problems, making it crucial to adopt a different strategy. To ensure quality assurance, two key areas can be targeted. Firstly, the process itself needs to be qualified, meaning that the PBF-LB/M machine must be certified for manufacturing parts for the construction industry. This qualification ensures that the company producing PBF-LB/M parts is capable of doing so in a reliable and controlled manner. Secondly, design restrictions should be implemented during the geometry optimization phase. By considering design restrictions, such as minimizing overhanging structures like holes, the potential for increased porosity at these critical areas can be reduced. For instance, topology optimization techniques often introduce holes into the parts, while shape optimization techniques do not. By focusing on process qualification and incorporating design restrictions during geometry optimization, the overall quality of PBF-LB/M parts can be effectively controlled. This approach addresses the economic challenges of certifying every unique part while also targeting the issue of porosity, particularly in relation to fatigue problems.

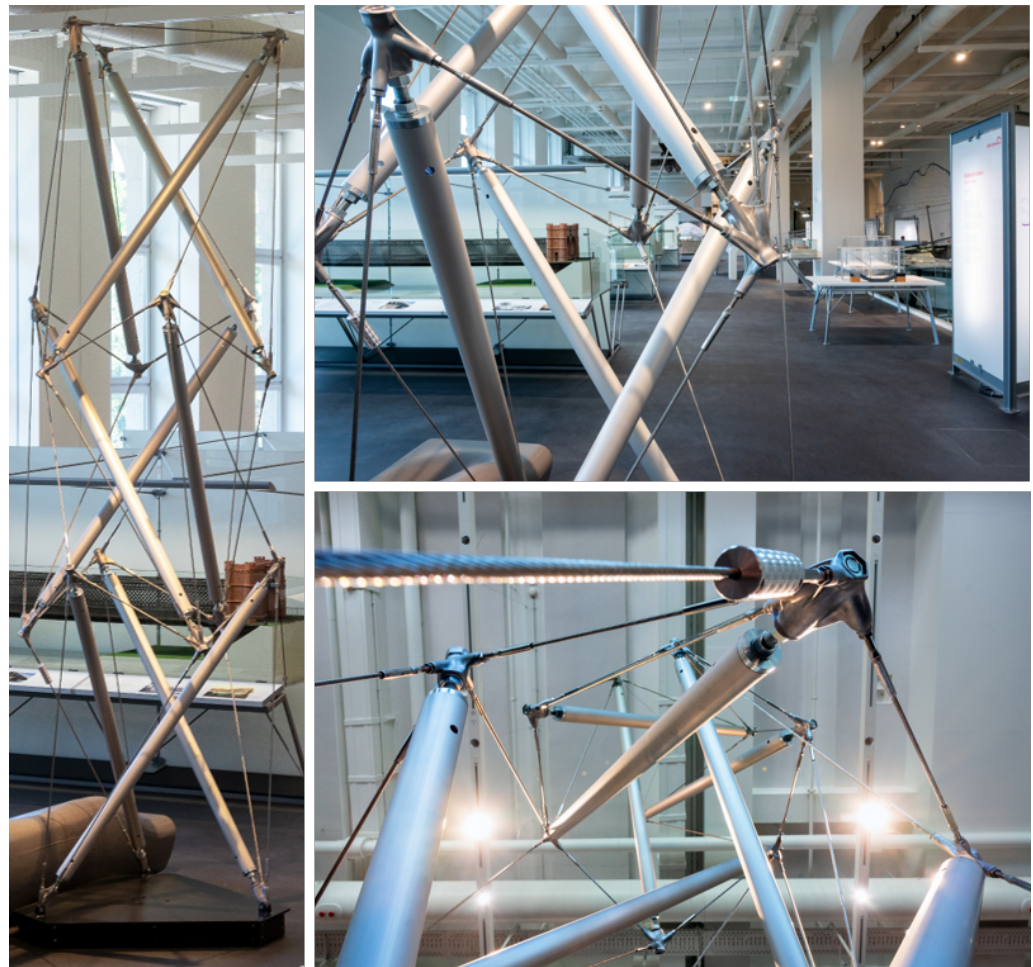


Figure 7. Assembled tensegrity tower with PBF-LB/M-manufactured connection nodes between the cables and the compression rods.

5. Conclusions and Outlook

From this study, the following conclusions can be drawn:

- The PBF-LB/M process was successfully integrated into the construction design process.
- A design and manufacturing route was proposed to safely implement the PBF-LB/M process into the construction design and manufacturing process.
- Shape optimization can be used to optimize the force flow in the part and reduce mass for faster production.
- A qualification method for PBF-LB/M machines for the construction sector is necessary, which is comparable to qualification methods of welding processes.
- Design restrictions should be implemented into the shape optimization process to reduce the danger of internal defects occurring.

Author Contributions: Conceptualization, J.D. and D.S.; methodology, J.D.; software, F.O.; validation, J.D. and J.B.; formal analysis, C.R.; investigation, J.D.; resources, M.M.; data curation, J.D. and D.G.; writing—original draft preparation, J.D.; writing—review and editing, D.S. and C.R.; visualization, J.D.; supervision, M.M.; project administration, C.R.; and funding acquisition, C.R. and J.D. All authors have read and agreed to the published version of the manuscript.

Funding: This study was funded by the Deutsche Forschungsgemeinschaft (DFG, German Research Foundation)—project number 414265976 – TRR 277. We would like to extend our sincere appreciation to the DFG for their invaluable funding and support towards the successful completion of this project.

Informed Consent Statement: Not applicable.

Data Availability Statement: Data available on request.

Acknowledgments: The authors would like to express their gratitude to Roesler Oberflächentechnik GmbH and Hausmann GmbH & Co. Stahlbau KG for their valuable collaboration in this study.

Conflicts of Interest: The authors declare no conflict of interest.

References

1. Schober, H.; Kürschner, K.; Jungjohann, H. Neue Messe Mailand– Netzstruktur und Tragverhalten einer Freiformfläche. *Stahlbau* **2004**, *73*, 541–551. [CrossRef]
2. Klahn, C.; Meboldt, M.; Fontana, F.F.; Leutenecker-Twelsiek, B.; Jansen, J. *Entwicklung und Konstruktion für die Additive Fertigung: Grundlagen und Methoden für den Einsatz in Industriellen Endkundenprodukten*; Vogel Business Media: Wuerzburg, Germany, 2021.
3. Hojjat, M.; Stavropoulou, E.; Bletzinger, K.U. The Vertex Morphing method for node-based shape optimization. *Comput. Methods Appl. Mech. Eng.* **2014**, *268*, 494–513. [CrossRef]
4. Yu, Z.; Dai, H.; Shi, Z. Structural form-finding of bending components in buildings by using parametric tools and principal stress lines. *Front. Archit. Res.* **2022**, *11*, 561–573. [CrossRef]
5. Diller, J.; Rier, L.; Siebert, D.; Radlbeck, C.; Krafft, F.; Mensinger, M. Cyclic plastic material behavior of 316L manufactured by laser powder bed fusion (PBF-LB/M). *Mater. Charact.* **2022**, *191*, 112153. [CrossRef]
6. Ghantasala, A.; Diller, J.; Geiser, A.; Wenzler, D.; Siebert, D.; Radlbeck, C.; Wüchner, R.; Mensinger, M.; Bletzinger, K.U. Node-based shape optimization and mechanical test validation of complex metal components and support structures, manufactured by laser powder bed fusion. In *Advances in Manufacturing, Production Management and Process Control*; Lecture Notes in Networks and Systems; Springer International Publishing: Cham, Switzerland, 2021; pp. 10–17.
7. Asl, R.N.; Shayegan, S.; Geiser, A.; Hojjat, M.; Bletzinger, K.U. A consistent formulation for imposing packaging constraints in shape optimization using Vertex Morphing parametrization. *Struct. Multidiscip. Optim.* **2017**, *56*, 1507–1519. [CrossRef]
8. Ingenieure, V.D. *Additive Manufacturing Processes-Powder Bed Fusion of Metal with Laser Beam (PBF-LB/M)-Material Data Sheet Aluminium Alloy AlSi10Mg*, 2nd ed.; Verband Deutscher Ingenieure: Bonn, Germany, 2020. Available online: <https://www.beuth.de/en/technical-rule/vdi-3405-blatt-2-1/326385793> (accessed on 15 May 2023).
9. Padovano, E.; Badini, C.; Pantarelli, A.; Gili, F.; D’Aiuto, F. A comparative study of the effects of thermal treatments on AlSi10Mg produced by laser powder bed fusion. *J. Alloys Compd.* **2020**, *831*, 154822. [CrossRef]
10. Li, Z.; Cheng, C.C.; Dhillon, J.S.; Kwon, S.Y.; Hudon, P.; Brochu, M. Precipitation behavior of an Al7SiMg alloy processed by laser powder bed fusion during non-isothermal and isothermal heat treatments. *Materialia* **2023**, *28*, 101751. [CrossRef]
11. Schneider, M.; Bettge, D.; Binder, M.; Dollmeier, K.; Dreyer, M.; Hilgenberg, K.; Klöden, B.; Schlingmann, T.; Schmidt, J. Reproducibility and Scattering in Additive Manufacturing: Results from a Round Robin on PBF-LB/M AlSi10Mg Alloy. *Pract. Metallogr.* **2022**, *59*, 580–614. [CrossRef]
12. Kan, W.H.; Nadot, Y.; Foley, M.; Ridosz, L.; Proust, G.; Cairney, J.M. Factors that affect the properties of additively-manufactured AlSi10Mg: Porosity versus microstructure. *Addit. Manuf.* **2019**, *29*, 100805. [CrossRef]
13. Aboulkhair, N.T.; Everitt, N.M.; Ashcroft, I.; Tuck, C. Reducing porosity in AlSi10Mg parts processed by selective laser melting. *Addit. Manuf.* **2014**, *1–4*, 77–86. [CrossRef]

Disclaimer/Publisher’s Note: The statements, opinions and data contained in all publications are solely those of the individual author(s) and contributor(s) and not of MDPI and/or the editor(s). MDPI and/or the editor(s) disclaim responsibility for any injury to people or property resulting from any ideas, methods, instructions or products referred to in the content.